

PROTON TRANSPORT THROUGH NON-HOMOGENEOUS VOXEL STRUCTURES.

J. G. Hunt, A. B. de Carvalho Jnr.
Institute of Radiation Protection and Dosimetry
Av. Salvador Allende s/n, Recreio, Rio de Janeiro.
CEP 22780 -160, Brazil.
john @ird.gov.br; alberico@ird.gov.br

ABSTRACT

The Monte Carlo code Visual Monte Carlo (Visual MC) written for photon transport through voxel structures was modified to transport protons through the same structures. Vavilov's approach to calculating the energy loss distribution was used. The energy deposited in each voxel was calculated. The angular distribution of multiple scattered protons was obtained using Highland's formula. Non-elastic nuclear interactions were simulated using the relevant cross-sections of the voxel material. The proton transport was first used in a voxel phantom simulating water, for various initial proton energies. The energy deposited along the beam center-line as a function of distance and the scattering at certain distances were compared with experimental data taken from the literature, and compared well. Following this, the proton transport code was run through the eye and compensator phantom used in the Quados intercomparison for protons, where it also compared well with the reference values. The code was then run using the Zubal voxel head phantom, to evaluate the possibility of its use in the area of dose calculation for proton radiotherapy. The graphics interface and the easy of use of the Windows program make the code very user-friendly.

Key Words: Proton transport, voxels, Monte Carlo, dose calculation.

1 INTRODUCTION

Proton transport Monte Carlo codes were first elaborated by Berger[1,2,3] in 1993 who also conducted experimental work to validate the code PTRAN. Later, a number of codes were written to transport protons through non-homogeneous structures, such as GEANT4, MCNPX, SRNA-2KG[4] and FLUKA-2002[5]. Applications of proton transport algorithms include radiotherapy with protons, computer tomography using protons and dose calculations for environments in which proton radiation fields exist. The advantages of proton therapy include the delivery of a high dose to the tissues under treatment, while preserving the adjacent tissues.

The Monte Carlo program VMC, written originally for photon transport through voxel structures[6,7] was modified to also simulate the transport of charged particles through voxel structures. The simulation of the transport of electrons, alpha particles and protons has been incorporated into the program. This paper relates the work done to permit the Monte Carlo transport of protons, and the validation of the results. The modified program was called VMCP, which will hopefully contribute to the overall understanding of charged particle transport.

VMCP was written in Visual Basic, which operates on the Windows® operating system, and has a number of advantages as to the ease of the set-up and operation of the code. The graphic interface allows the phantoms used to be visualized and all stages of the proton transport to be shown.

2 VMCP PROTON TRANSPORT

Protons traversing matter lose energy through successive collisions with the atoms and molecules of the material. With respect to energy loss, the most important interaction is between the proton and the atomic or molecular electrons. The interaction between a proton and an atomic nucleus (nuclear reactions) also has to be taken into account. The most important parameter characterizing the energy loss of an incident proton is the stopping power, which is mean energy loss per unit path length in a material. The stopping powers used in VMCP were obtained from ICRU 49[8]. The CSDA (Continuous Slowing Down Approximation) range may be obtained by integrating the inverse of the stopping power from zero proton energy to the initial proton energy. The CSDA ranges are also tabled in the ICRU document.

2.1 Energy and Range Straggling

The amount of energy transferred from a proton to an atomic electron, as well as the number of interactions that occur per unit path length has a probability distribution. This causes statistical fluctuations in the energy deposition. In VMCP, the Valilov energy distribution function was treated in a numerical way to produce a gaussian distribution for the range of individual protons:

$$r = r_o + \sigma(r_o)\xi \quad (1)$$

where r_o is CSDA range calculated with data taken from ICRU 49, ξ is gaussian distribution given by:

$$\xi = \sin(2\pi z_1)\sqrt{-2\log(z_2)} \quad (2)$$

and $\sigma(r_o)$ is the standard deviation in position of protons at the depth and r_o the CSDA range:

$$\sigma(r_o) = 0.012r_o^{0.956} \quad (3)$$

2.2 Proton Multiple Scattering

A proton will experience a deflection as it passes in the neighborhood of a nucleus. This deflection is the result of the combined interaction with the Coulomb- and hadronic field of the nucleus (the deflection caused by collisions with electrons can be neglected because of the mass ratio). This cross section decreases very rapidly with increasing angle, and with increasing energy. The consequence is that most particles are only slightly deflected. However, the effect of multiple scatterings is that the proton's direction can be changed through a large angle, especially at the end of the trajectory when the proton energy is quite low. In VMCP, the passage of the proton through each voxel was considered to be one step, Highland's formula[9] was used to calculate the scattering at each step:

$$\theta_0 = \frac{14,1}{p\beta c} z \sqrt{\frac{L}{L_R}} \quad (4)$$

where p is the momentum of the proton, βc is its velocity in the reference frame of the laboratory, z is the charge on the proton, L is the step length and L_R is the radiation length of the proton in the material. After each step the new direction cosines of the proton were re-evaluated.

2.3 Proton Interaction with Nuclei

Because the energy of the proton in radiotherapy applications is much higher than the Coulomb-barrier, protons have a probability of reacting with the nucleus. This causes a decrease of the proton flux with depth, already long before the end of the proton range. The average number of interactions on proton step Δz is calculated according to the following relation:

$$\mu_{nuc}(\bar{E}) = \frac{N_0}{A} \sigma(\bar{E}) \cdot \Delta z \quad (5)$$

where N_0 is Avogadro's number, A is the atomic weight of the nuclei, Δz is the size of the step and $\sigma(E)$ is a cross section for oxygen. The cross sections were taken from ICRU 63[10]. Figure 1 shows the cross section of ^{16}O as a function of proton energy.

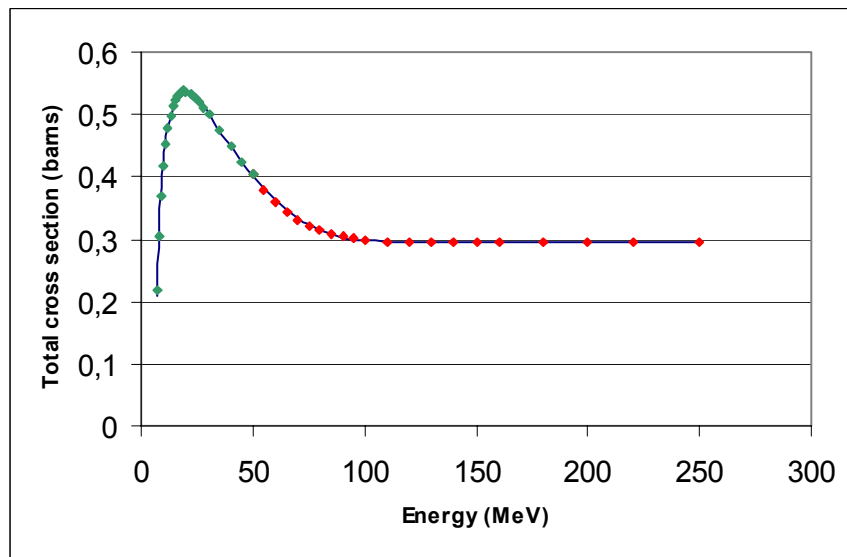


Figure 1 – The total cross section for nuclear reactions in ^{16}O .

With respect to the reaction products, the situation is more complicated. The secondary particles can be neutrons, protons and recoil fragments. The energy transferred to the recoil fragments will be deposited locally, but secondary protons can travel a considerable distance before stopping. The secondary neutrons will either escape from the medium or produce another nuclear reaction, in which tertiary particles can be produced. In VMCP, the approximation used by Seltzer was applied, whereby the energy of secondary charged particles is considered to be

deposited locally, and the secondary uncharged particles are assumed to leave the material without further depositing energy along the proton tracks. Seltzer defined a function $\eta(E)$, which represents the fraction of energy imparted to charged particles after a nuclear reaction at proton energy E in water. Figure 2 shows the graph total fraction of incident proton energy transferred in nonelastic nuclear collisions to all charged particles.

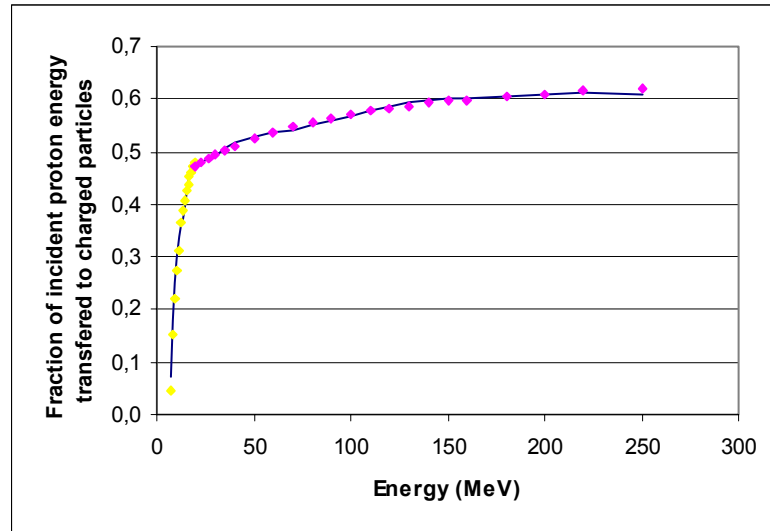


Figure 2 – The total fraction of incident proton energy transferred in non-elastic nuclear collisions to all charged particles.

3 VALIDATION OF VMCP

3.1 Proton Transport in Water

The proton transport through water was simulated, calculating the dose distribution as a function of depth in water for the initial proton energies of 158.5, 188.4 and 214.5 MeV. The results obtained, normalized by the maximum value, were compared to the experimental results given by Berger [3]. The differences between the experimental values and the calculated values are less than 2% in the region of the Bragg peak. Figure 3 shows the results of the simulation of the transport of 214.5 MeV protons through water. A water phantom made of voxel of side 2 mm was used. The protons were emitted in a pencil beam of radius 5 cm.

The simulation of the radial scattering of protons in water was made using the same water voxel phantom. Protons were emitted in a very thin pencil beam with an initial energy of 127 MeV. At three depths in water, the proton fluence was binned as a function of the radial distance from the center of the beam. Figure 4 shows the angular distribution of multiple scattered protons in water. The radial distance at which the beam intensity fell to 0.368 ($1/e$) of the maximum was verified, and compared with the experimental values of Berger. The comparison of the calculated and simulated values is shown in Table 1.

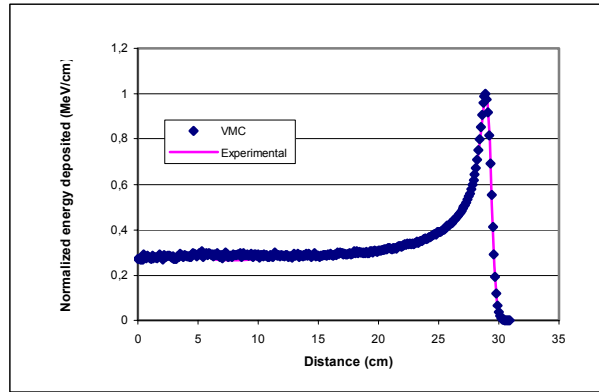


Figure 3. Transport of 214.5 MeV protons in water. Comparison of depth dose curves measured experimental and calculated with VMCP.

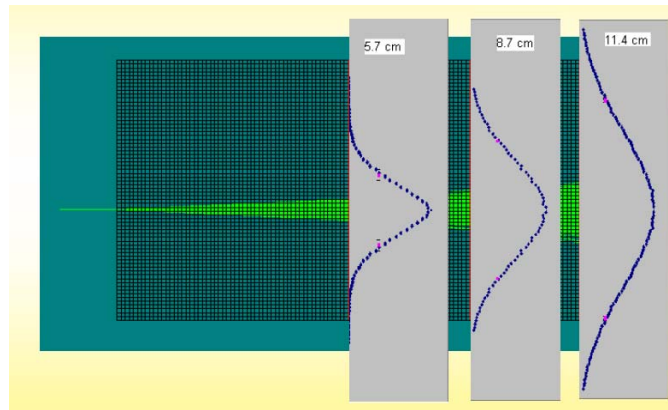


Figure 4 – 127 MeV protons -angular distributions of multiple scattered protons at three distances in water.

Table 1. Comparison of experimental and VMCP results for radial scattering of a 127 MeV pencil proton beam.

Depth in water (cm)	Radial distance for $I_{max}/0.368$ (mm)	
	Experimental	VMCP
5.7	1.15 ± 0.15	1.068
8.7	2.18 ± 0.10	2.175
11.4	3.46 ± 0.09	3.537

3.2 Proton Transport through Non-homogeneous Voxel Phantoms

The proton transport question in the QUADOS (Quality Assurance of Computational Tools for Dosimetry)[11] was used to compare the VMCP transport with the proton transport simulated using other Monte Carlo programs. The QUADOS phantom consisting of a PMMA compensator followed by a spherical water phantom simulating the human eye was introduced into VMCP. A voxel size of $0.5 \times 0.5 \times 0.5 \text{ mm}^3$ was used. Dose distributions were calculated for a disk source of radius 7.5 mm for firstly a mono-energetic proton beam of initial energy of 50 MeV and secondly a proton beam with initial energies between 40 and 50 MeV which simulate a modulated proton beam. Figure 5 shows the phantom geometry as shown in VMCP and Figure 6 shows the comparison of VMCP results with QUADOS results.

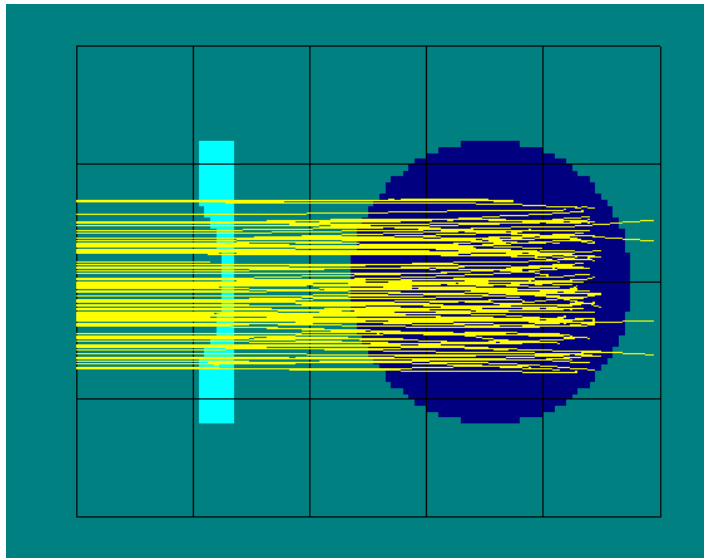


Figure 5 -Set up for irradiation in QUADOS - VMCP for proton energy 40-50 MeV.

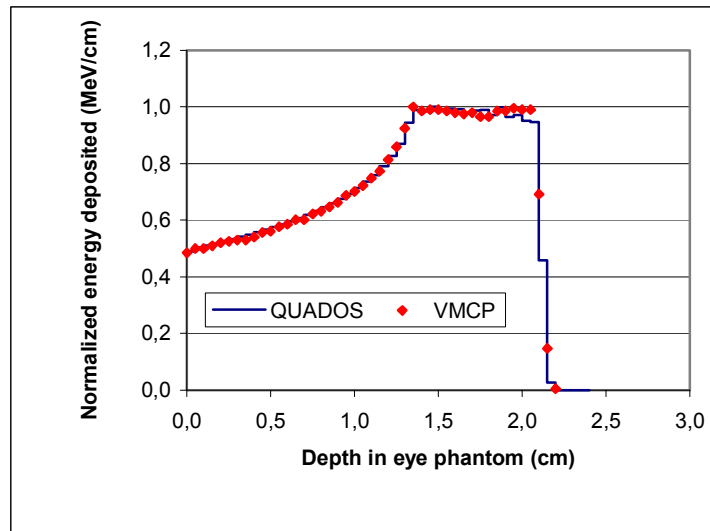


Figure 6 -Comparison of depth dose curve calculated QUADOS and VMCP for proton energy 40-50 MeV.

3.3 Proton Transport through Anthropomorphic Phantoms

The voxel phantom of the head produced from an MRI by Zubal[12] was used to simulate the proton transport through anthropomorphic structures. The segmented head phantom has a voxel size of $0.11 \times 0.11 \times 0.14 \text{ cm}^3$. The isodose curves for a modulated 50 MeV proton beam as in the QUADOS example are shown in Figure 7.

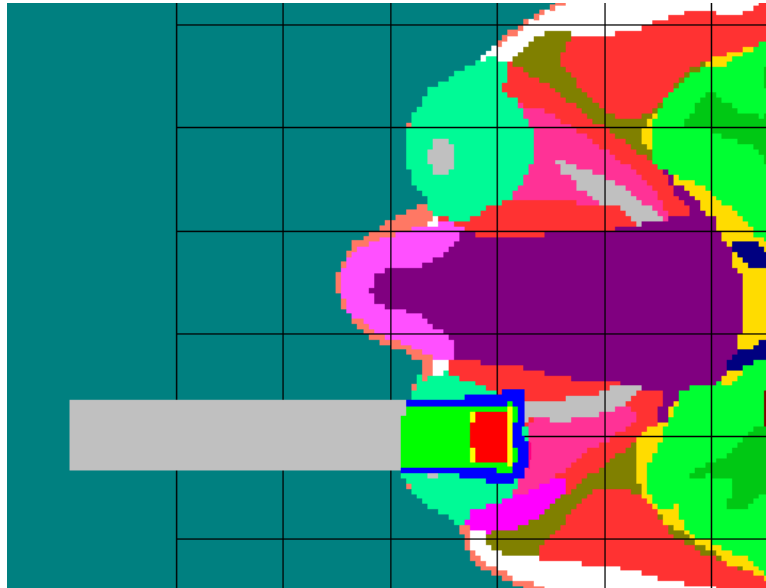


Figure 7 – Dose distribution of proton beam of 40-50 MeV in voxel phantom of the head.

The comparisons of VMCP results with experimental results or results from other Monte Carlo programs shows that the program can be used to calculate dose deposition in non-homogeneous voxel structures with an uncertainty of less than 5%. It is planned to continue the elaboration of the program to reduce further the uncertainties and to improve the user interface.

4 ACKNOWLEDGMENTS

Financial support for the work presented here was provided by FAPERJ. This work was carried out at the IRD as part of the requirement for the obtention of a master's thesis in radiation protection.

5 REFERENCES

1. M. J. Berger, "Proton Monte Carlo transport program PTRAN", *NIST Report NISTIR 5113*, (1993a).
2. M. J. Berger, "Penetration of proton beams through water I. Depth-dose distributions, spectra and LET distributions", *NIST Report NISTIR 5226*, (1993b).

3. M. J. Berger, “Penetration of proton beams through water II. Three-dimensional absorbed dose distributions”, *NIST Report NISTIR 5330*, (1993c).
4. R.D. Ilic, “SRNA-2KG - Proton Transport Simulation by Monte Carlo Techniques”, *Institute of Nuclear Sciences, Vinca, Phys. Lab.*, (010), Beograd, Yugoslavia, February, (2002).
5. A. Fasso, A. Ferrari, J. Ranft, and P. R. Sala, “FLUKA: Status and Prospective for Hadronic Applications,” in *Advanced Monte Carlo for Radiation Physics, Particle Transport Simulation and Applications, Proceedings of the Monte Carlo 2000 Conference, Lisbon, October 23–26, 2000*, edited by A. Kling, F. Barao, M. Nakagawa, L. Tavora, and P. Vaz. Springer-Verlag, Berlin, pp.955–960 (2000).
6. J.G. Hunt, F.C.A da Silva, D.S. dos Santos, I. Malatova, B.M. Dantas, A. Azeredo. “Visual Monte Carlo and its Application to Internal and External Dosimetry,” in *Advanced Monte Carlo for Radiation Physics, Particle Transport Simulation and Applications, Proceedings of the Monte Carlo 2000 Conference, Lisbon, October 23–26, 2000*, edited by A. Kling, F. Barao, M. Nakagawa, L. Tavora, and P. Vaz. Springer-Verlag, Berlin, pp.345-350 (2000).
7. J.G. Hunt, F.C.A da Silva, C.L.P. Mauricio, D.S. dos Santos. “The validation of organ dose calculations using voxel phantoms and Monte Carlo methods applied to point and water immersion sources”. *Radiat. Prot. Dosim.* **108** (1), pp.85-89 (2004).
8. ICRU Report 49, “Stopping Powers and Ranges for Protons and Alpha Particles”, *International commission on radiation units and measurements* Washington DC, (1993).
9. B. Gottschalk, A. M. Koehler, Schneider, *et al.*, “Multiple Coulomb Scattering of 160 MeV Protons”, *Nuc. Instr. and Meth. in Physics Research B*, v. 74, pp. 467-420 (1993).
10. ICRU Report 63, “Nuclear Data for Neutron and Proton Radiotherapy and for Radiation Protection”, *International commission on radiation units and measurements* Washington DC, (2000).
11. QUADOS. “Intercomparison on the usage of computational codes in radiation dosimetry”. www.nea.fr/download/quados/quados.html. Bologna, Italy, 14 - 16 July (2003).
12. I. G. Zubal, C. R. Harrell, E. O. Smith. “A computerized three-dimensional segmented human anatomy” *Med. Phys.* **21** pp.299–302 (1994).